NUCLEAR THEORY, Vol. 29 (2010)
eds. A. Georgieva, N. Minkov, Heron Press, Sofia

Extended Microscopic Theory for Medium-Mass Nuclei – Basics, First Results, Future

K.P. Drumev[1,2], **J.P. Draayer**[2]

[1]Institute of Nuclear Research and Nuclear Energy, Bulgarian Academy of Sciences, Sofia 1784, Bulgaria
[2]Department of Physics and Astronomy, Louisiana State University, Baton Rouge, LA 70803, USA

Abstract. An extended SU(3) shell model that for the first time explicitly includes unique-parity levels is introduced. Its relevance is established by calculations with a realistic interaction performed for a group of upper fp-shell nuclei where valence nucleons beyond the N=28=Z core occupy levels of the normal parity upper-fp shell $(f_{5/2}, p_{3/2}, p_{1/2})$ and the unique parity $g_{9/2}$ intruder configuration. The levels of the upper fp-shell are handled within the framework of an m-scheme basis as well as its pseudo-SU(3) counterpart, and respectively, the $g_{9/2}$ as a single level and as a member for the complete gds shell. More detailed analyses are done for the waiting-point nuclei of ^{64}Ge and ^{68}Se which demonstrate that the extended SU(3) approach allows one to better probe the effects of deformation and to account for many key properties of the system by using a highly-truncated model space. The model holds promise to be useful for the rare-earth domain as well where many previous results can and will be complemented, revised and improved.

1 Introduction

Intruder levels are present in heavy deformed nuclei where the strong spin-orbit interaction destroys the underlying harmonic oscillator symmetry of the nuclear mean-field potential. The role they play for the overall dynamics of the system has been the topic of many questions and debates [1–4]. Until now, the problem has been either approached within the framework of a truncation-free toy model [1] or by just considering the role of the single intruder level detached from its like-parity partners [2, 3]. It was argued in [1] that particles in these levels contribute in a complementary way to building the collectivity in nuclei. However, some mean-field theories suggest that these particles play the dominant role in inducing deformation [4]. In order to build a complete shell-model theory, these levels need to be included in the model space especially if experimentally observed high-spin or opposite-parity states are to be described.

Until recently, SU(3) shell-model calculations - real SU(3) [5] for light nuclei and pseudo-SU(3) [6] for heavy nuclei - have been performed in either only

one space (protons and neutrons filling the same shell, e.g. the ds shell) or two spaces (protons and neutrons filling different shells, e.g. for rare-earth and actinide nuclei). Various results for low-energy features, like energy spectra and electromagnetic transition strengths, have been published over the years [7–9]. These applications confirm that the SU(3) model works well for light nuclei and the pseudo-SU(3) scheme, under an appropriate set of assumptions, for rare-earth and actinide species. Up to now, SU(3)-based methodologies have not been applied to nuclei with mass numbers $A = 56$ to $A = 100$, which is an intermediate region where conventional wisdom suggests the break down of the assumptions that underpin their use in the other domains. In particular, the $g_{9/2}$ intruder level that penetrates down from the shell above due to the strong spin-orbit splitting appears to be as spectroscopically relevant to the overall dynamics as the normal-parity $f_{5/2}, p_{3/2}, p_{1/2}$ levels. Specifically, in this region the effect of the intruder level cannot be ignored or mimicked through a "renormalization" of the normal-parity dynamics which is how it has been handled to date.

We introduce and establish the benefits of a new and extended SU(3) shell model which, for the first time, explicitly includes particles from the complete unique-parity sector and therefore can be used to explore the role that intruder levels play in the dynamics of the system. Calculations are performed for two nuclei which are of major importance in astrophysics, namely, the waiting-point $N = Z$ nuclei ^{64}Ge and ^{68}Se [10]. In addition, ^{68}Se is known to be among the nuclei for which shape coexistence effects have been reported [11, 12]. Both the strengths and the limitations of the model are demonstrated and discussed.

2 A Reasonable Approach for the Description of Upper fp-Shell Nuclei

To benchmark the benefit of the SU(3) scheme in this region (pseudo-SU(3) for the upper-fp shell and normal SU(3) for the $g_{9/2}$ configurations extended to the full gds shell), we first generated results in a standard m-scheme representation [13] for both nuclei, ^{64}Ge and ^{68}Se, with the 8 (4 protons + 4 neutrons) and 12 (6 protons + 6 neutrons) valence nucleons, respectively, distributed across the $p_{1/2}, p_{3/2}, f_{5/2}, g_{9/2}$ model space with the $f_{7/2}$ level considered to be fully occupied and part of a ^{56}Ni core. The Hamiltonian we used is a G-matrix with a phenomenologically adjusted monopole part [14, 15] that in many cases describes the experimental energies reasonably well. Specifically, this upper-$fp + g_{9/2}$ shell interaction was succesfully used in the past to obtain quite good results for nuclei like ^{62}Ga [16], and ^{76}Ge and ^{82}Se [14]. Later, it was applied for exploring the pseudo-SU(4) symmetry in the region from the beginning of the upper fp-shell up to $N = 30$ and for describing beta decays [17].

Calculations with different cuts of the full model space were done in order to estimate the occupancy of the single-particle levels and thus to evaluate the relative importance of various configurations for describing essential nuclear characteristics. In Figure 1, a comparison is made between the occupancies for

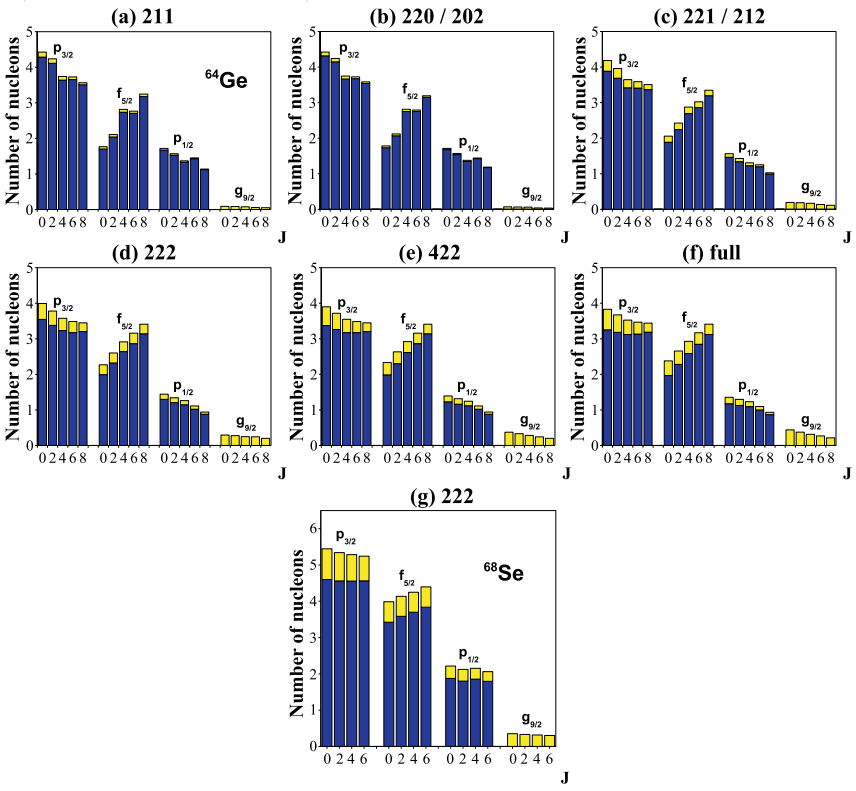

Figure 1. Single-particle occupation numbers for eigenstates of the g.s. band of ^{64}Ge (calculated in different restricted model spaces (from (a) to (e)) and the full space (f)) and ^{68}Se in a restricted model space (g). The labels TPN over each restricted-space calculation represent the maximum total number of particles T, and the maximum number of protons P (and neutrons N) allowed in the intruder $g_{9/2}$ level.

^{64}Ge and ^{68}Se as determined in various restricted spaces, where different number of particles are allowed in the $g_{9/2}$ level and the full-space resuls. The upper (yellow) bars show the contribution to occupations from basis states with an occupied intruder level while the lower (blue) portion represents those where the intruder level is empty. The calculated results suggest that the occupancy probability for the intruder level is approximately 0.3 particles for the low-lying states of both ^{64}Ge and ^{68}Se. Calculations with no particles allowed in the intruder level or with just one identical-particle (or proton-neutron) pair (Figure 1 (a) and (b)) cannot describe either its occupancy or the gradual change in the occupancy of the single-particle levels in the ground-state (g.s.) band that is found in the full-model-space results. However, using a restricted space with at most two identical particles occupying the intruder level (in Figures 1(e) and (g)) is

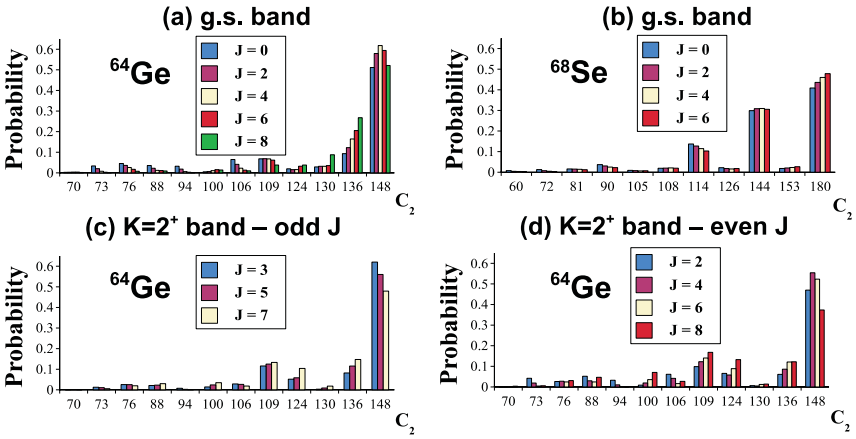

Figure 2. Pseudo-SU(3) content of the low-lying states in (a) the g.s. band of ^{64}Ge, (b) and (c) - the $K = 2^+$ band of ^{64}Ge, and (d) the g.s. band of ^{68}Se using the renormalized counterpart of the G-matrix realistic interaction.

sufficient to describe both features as well as the low-energy spectrum and the B(E2) transition strengths [18]. Similar results were observed for the $K = 2^+$ band of this nucleus. Calculations for ^{68}Se performed in a truncated basis with at most 2 nucleons allowed in the intruder level produce a slighlty higher value of the $g_{9/2}$ occupancy compared to ^{64}Ge as can be seen in Figure 1 (g).

Next, the goodness of the pseudo-SU(3) symmetry in these nuclei was tested using a renormalized version of the same realistic interaction in the $pf_{5/2}$ space [14]. The matrix of the second-order Casimir operator of pseudo-SU(3), $C_2 = \frac{1}{4}(3\hat{L}^2 + Q.Q)$, was generated and the method of moments [19] used to diagonalize this matrix by starting the Lanzcos procedure with specific eigenvectors of the Hamiltonian for which a pseudo-SU(3) decomposition was desired.

The distribution of the second order Casimir operator C_2 of pseudo-SU(3) yields contributions of about 50-60% from the leading pseudo-SU(3) irrep in the g.s. band of ^{64}Ge (Figure 2(a)) which suggests that the pseudo-SU(3) symmetry is quite good. In the $K = 2^+$ band (Figure 2 (c) and (d)) this contribution appears to be somewhat lower, ranging from approximately 37% for the 8_2^+ state to about 62% in the 3_1^+ state. The analysis also reveals that using only five irreps which have the highest C_2 value one may take account of at least 70% and up to about 95% of the wavefunction for the states in these bands.

In the case of ^{68}Se, the outcome turns out to be quite similar for the states from the g.s. band (Figure 2(b)). Although the irreps with the maximal value of $C_2 = 180$ participate with only between about 40% and 50%, the first eleven irreps with distinct values of λ and μ account for 88-93% of the wavefunction. In addition, the 0_3^+ state at 2.51 MeV is also dominated (64%) by irreps with the biggest C_2 value. However, other states are predicted to be highly-mixed SU(3)

configurations. This includes the 0_2^+ state found at 1.05 MeV – a value very similar to the ones reported in [11, 12] for a low-lying state of prolate shape. A recent analysis reveales that many low-lying states in other $N \sim Z$ nuclei also have good pseudo-SU(3) symmetry which further underscores the value of using symmetry-based truncation schemes [18].

3 An Extended SU(3) Model with Explicitly Included Intruder Levels

Following the series of arguments and motivations presented in the previous section, we can now introduce the basics of the extended SU(3) shell model. Like its early precursors [5, 6], it is also a microscopic theory in the sense that both SU(3) generators - the angular momentum ($L_\mu, \mu = 0, \pm 1$) and quadrupole ($Q_\mu; \mu = 0, \pm 1, \pm 2$) operators – are given in terms of individual nucleon coordinate and momentum variables. However, the model space has a more complicated structure than the one used in earlier models based on the SU(3) symmetry. Specifically, it consists of two parts for each particle type, a normal (N) parity pseudo-shell ($f_{5/2}, p_{3/2}, p_{1/2} \rightarrow \tilde{d}_{5/2}, \tilde{d}_{3/2}, \tilde{s}_{1/2}$) and a unique (or abnormal) (U) parity shell composed of all levels of opposite parity from the gds shell above.

The many-particle basis states

$$|\{a_\pi; a_\nu\}\rho(\lambda, \mu)\kappa L, \{S_\pi, S_\nu\}S; JM\rangle \tag{1}$$

are built as SU(3) proton (π) and neutron (ν) coupled configurations with well-defined particle number and good total angular momentum. Here, the proton and neutron quantum numbers are indicated by $a_\sigma = \{a_{\sigma N}, a_{\sigma U}\}\rho_\sigma(\lambda_\sigma, \mu_\sigma)$, where the $a_{\sigma\tau} = N_{\sigma\tau}[f_{\sigma\tau}]\alpha_{\sigma\tau}(\lambda_{\sigma\tau}, \mu_{\sigma\tau})$ are the basis-state labels for the four spaces in the model (σ stands for π or ν, and τ stands for N or U). In the last expression, $N_{\sigma\tau}$ denotes the number of particles in the corresponding space, $[f_{\sigma\tau}]$ - the spatial symmetry label and $(\lambda_{\sigma\tau}, \mu_{\sigma\tau})$ - the SU(3) irrep label. Multiplicity indices $\alpha_{\sigma\tau}$ and ρ_σ count different occurences of $(\lambda_{\sigma\tau}, \mu_{\sigma\tau})$ in $[f_{\sigma\tau}]$ and in the product $\{(\lambda_{\sigma N}, \mu_{\sigma N}) \times (\lambda_{\sigma U}, \mu_{\sigma U})\} \rightarrow (\lambda_\sigma, \mu_\sigma)$, respectively. First, the particles from the normal and the unique spaces are coupled for both protons and neutrons. Then, the resulting proton and neutron irreps are coupled to a total final set of irreps. The total angular momentum J results from the coupling of the total orbital angular momentum L with the total spin S. The ρ and κ are, respectively, the multiplicity indices for the different occurences of (λ, μ) in $\{(\lambda_\pi, \mu_\pi) \times (\lambda_\nu, \mu_\nu)\}$ and L in (λ, μ).

The Hamiltonian

$$\begin{aligned} H &= \sum_{\sigma,\tau}(H_{sp}^{\sigma\tau} - GS^{\sigma\tau\dagger}S^{\sigma\tau}) - \frac{\chi}{2} : Q.Q : + aJ^2 + bK_J^2 \\ &- G(\sum_{\sigma,\tau\neq\tau'} S^{\sigma\tau\dagger}S^{\sigma\tau'} + \sum_{\tau,\tau'} S^{\pi\nu,\tau\dagger}S^{\pi\nu,\tau'}) \end{aligned} \tag{2}$$

includes spherical Nilsson single-particle energies as well as the quadrupole-quadrupole and pairing interactions (within a shell and between shells) plus two rotor-like terms that are diagonal in the SU(3) basis. In first approximation, the quadrupole operator in the normal-parity spaces is related to its pseudo counterpart by $Q_{\sigma N} \approx \frac{\tilde{\eta}+1}{\tilde{\eta}} \tilde{Q}_{\sigma N}$ with $\tilde{\eta}$ equal to 2 for both protons and neutrons and $Q = Q_{\pi N} + Q_{\pi U} + Q_{\nu N} + Q_{\nu U} \approx 1.5\ \tilde{Q}_{\pi N} + Q_{\pi U} + 1.5\ \tilde{Q}_{\nu N} + Q_{\nu U}$.

The second line in Eq.(2) consists of pairing terms that are included for the first time in SU(3) shell-model calculations. In particular, the first term represents the scattering of an identical-particle pair between the normal- and unique-parity spaces. The second one stands for the proton-neutron pairing (or simply pn-pairing) interaction within the normal- or unique-parity space (terms with $\tau = \tau'$) and for the pn-pair scattering between the normal- and unique-parity spaces (terms with $\tau \neq \tau'$). Finally, the two rotor-like terms J^2 and K_J^2 (the square of the total angular momentum and its projection on the intrinsic body-fixed axis) are used to "fine tune" the energy spectra, adjusting the moment of inertia of the g.s. band and the position of the $K = 2^+$ bandhead, respectively. Their strengths are the only two parameters fitted in this work.

The single-particle terms together with the proton, neutron and proton-neutron pairing interactions mix the SU(3) basis states, which allows for a realistic description of the energy spectra of the nuclei. The single-particle energies in the Hamiltonian for the normal spaces are fixed with the numbers provided by the upper-fp shell single-particle energies and for the strengths in the unique-parity spaces the numbers from systematics are used [20]. The values for the parameters G and χ in the Hamiltonian which are taken from [21] are found to be in agreement with the ones [20, 22] used in previous calculations for some ds-shell and rare-earth nuclei. For simplicity, we take both identical-particle and proton-neutron pairing strengths to be equal.

4 Results and Discussion

Calculations within the framework of the extended SU(3) model were performed using irreps from 5 types of configurations - for example, $[N_{\pi N}, N_{\pi U}; N_{\nu N}, N_{\nu U}]$ = $[4,0;4,0]$, $[4,0;2,2]$, $[2,2;4,0]$, $[3,1;3,1]$ and $[2,2;2,2]$ for the ^{64}Ge case. For each of these groups, irreps in the proton and neutron spaces with (pseudo-) spin $S_{\sigma\tau} = 0,\ 1/2,\ 1$ and $3/2$ in both the normal- and the unique-parity spaces were generated. Then, from all the possible couplings between these we chose those with the largest value of the second order Casimir operator of SU(3) and spin $S = 0$, 1 and 2. Here, we present results obtained with five (seven) coupled proton-neutron irreps with distinct values of λ and μ for each distribution of particles between the normal and unique spaces for ^{64}Ge (^{68}Se). (This number was even pushed up to eleven for the [6,0;6,0] configuration in ^{68}Se). The complete set consists of $492\ (580)$ coupled irreps in the case of ^{64}Ge (^{68}Se).

For both ^{64}Ge and ^{68}Se, proton-neutron configurations with no particles in the unique space are found, as expected, to lie lowest and determine, by-

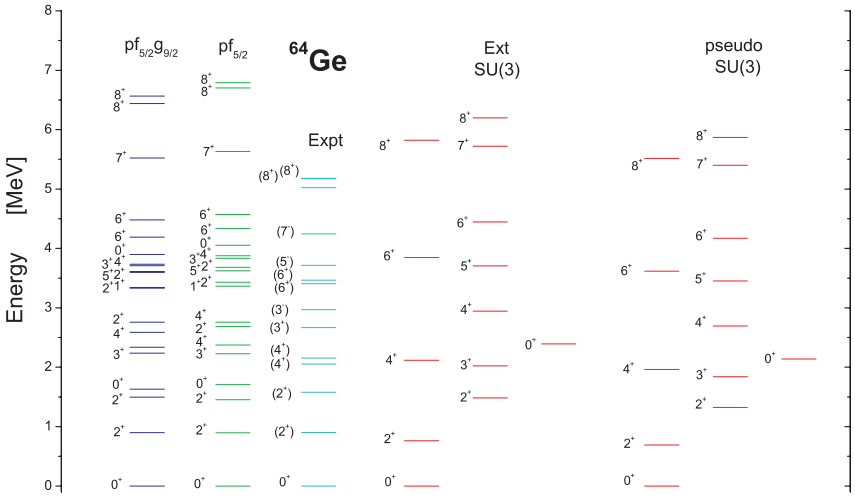

Figure 3. Low-energy spectra of ^{64}Ge obtained with (from left to right) the realistic interaction in the full $pf_{5/2}g_{9/2}$ and $pf_{5/2}$ model spaces compared with experiment [23] and the extended-SU(3)- and the pseudo-SU(3)-model results.

and-large, the structure of the low-lying eigenstates. Only a small portion of all proton-neutron coupled irreps - 27 (112) in the case of ^{64}Ge (^{68}Se) - belong to these types of configurations, which we will refer to as the dominant ones. Since the only possible irrep in the unique-parity spaces for this case is $(\lambda_{\pi U}, \mu_{\pi U}) = (0, 0)$ (and $(\lambda_{\nu U}, \mu_{\nu U}) = (0, 0)$), these configurations are the exact pseudo analog of the ones encountered in the ds-shell nuclei ^{24}Mg and ^{28}Si which have been studied earlier [7]. Using only the principal part of the Hamiltonian (2), namely, the part with both rotor term strengths equal to zero, we are able to provide a good description of the low-lying states. Specifically, all the energies from the g.s. bands (with the exception of the 2_1^+ state in ^{68}Se) differ by no more than 15% from the experimental values [23]. In order to conform with this result and prevent any further changes in the structure of the wave function, the range of values for the parameters a and b were severely restricted so that these terms only introduce small ("fine tuning") changes to the overall fit.

Results for the excitation spectra of ^{64}Ge are presented in Figure 3. The realistic G-matrix interaction gives a reasonable result for the low-lying states consistent with the one obtained in [11, 21]. Moreover, a description of a similar quality is provided by the extended SU(3) model. The existence of two prolate bands, as predicted by the calculations with the realistic interactions, is also observed, that is, a g.s. $K = 0^+$ and an excited $K = 2^+$ band, both dominated by the $(8, 4)$ irrep. The first excited 0^+ (0_2^+) state, not reported yet experimentally, is found at 2.39 MeV which is higher than the prediction made by the realis-

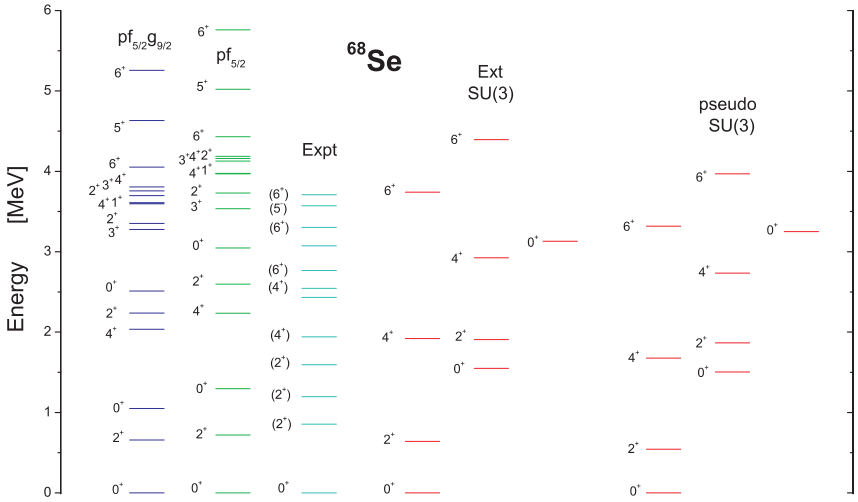

Figure 4. Low-energy spectra of ^{68}Se obtained with (from left to right) the realistic interaction in the restricted $pf_{5/2}g_{9/2}$ (at most 2 particles allowed in the intruder $g_{9/2}$ level) and full $pf_{5/2}$ model spaces compared with experiment [23], the extended-SU(3)- and the pseudo-SU(3)-model results.

tic interactions. Result from the pseudo-SU(3) model, shown also in the figure, does not seem to differ signifficantly.

A slight change in the type of Hamiltonian used helps us establish the transition from states of prolate shape dominated by the irrep (12,0) in the g.s. band to ones where the (0,12) irrep prevails. To achieve this effect we need to add a term proportional to the third order Casimir invariant C_3 of SU(3). It was demostrated earlier [7] that this term is capable of adjusting the prolate-oblate band crossing by driving irreps with $\mu >> \lambda$ lower in energy than those with $\lambda >> \mu$. The same term can also be used to fix the position of the first excited 0^+ (0_2^+) state not assigned yet experimentally but predicted by our G-matrix calculations to lie at 1.05 MeV.

Consistent with the outcome for ^{64}Ge, in the case of ^{68}Se we found a reasonable description for the energies of the states from the g.s. band (Figure 4). Even the use of a restricted space with at most 2 nucleons allowed in the intruder $g_{9/2}$ level produces result which reflects some basic characterisics of the full-space spectrum reported in [11]. For example, the first excited 0^+ state (0_2^+) is also positioned below the 2_2^+ state. A new feature observed in our results is that the 0_3^+ state at 2.51 MeV was found to be dominated by the shapes with $C_2 = 180$. Within the framework of the extended SU(3) shell model, ^{68}Se is a mid-shell nucleus, a fact which may explain the shape coexistence effects. Unlike the case of ^{28}Si [7], now the g.s. band is dominated by the irrep $(12, 0)$, if the C_3 term is not included in the Hamiltonian. This result, which corresponds to a prolate shape

mainly follows due to the role of the orbit-orbit terms. If C_3 is included then we obtain result dominated by the irrep $(0, 12)$ which is in agreement with some earlier discussions [24, 25]. Because of the nature of the leading representation, the model can not easily account for a $K = 2^+$ band with the same shape characteristic, neither can it give a simple explanation for a low-lying $K = 0^+$ band, facts which are in support of the realistic prediction made for a highly-mixed nature of the 0_2^+ as well as some other low-lying states in this nucleus.

Electromagnetic transition strengths are normally calculated with the E2 transition operator of the form [3, 26]:

$$\begin{aligned} T(E2) &\approx \sqrt{5/16\pi}A^{1/3}(e_\pi \frac{\tilde{\eta_\pi}+1}{\eta_\pi}\tilde{Q}_{\pi N} + e_\pi Q_{\pi U} \\ &+ e_\nu \frac{\tilde{\eta_\nu}+1}{\eta_\nu}\tilde{Q}_{\nu N} + e_\nu Q_{\nu U}) \end{aligned} \quad (3)$$

Instead, in this work we simply used the single dominant component in the pseudo-SU(3) expansion of the quadrupole operators in the normal-parity space. The effective charges e_π and e_ν were taken as $e_\pi = 1.5$ and $e_\nu = 0.5$ for the two versions of the realistic interaction and the extended-SU(3) calculations. The overall agreement between the results for both nuclei (see Table 1) is good, although some recent experimental findings for the $2^+_{g.s.} \rightarrow 0^+_{g.s.}$ transition strength in ^{64}Ge [27] seem to be underestimated by approximately a factor of 1.4. The correct behavior of the interband transitions is also nicely reproduced. More significant deviations are observed for the transitions between members of the $K = 2^+$ band and the $(J + 1)^+ \rightarrow J^+$ transitions in ^{64}Ge. These could be

Table 1. Intraband B(E2) transition strengths for ^{64}Ge and ^{68}Se in units of e^2fm^4 calculated using the G-matrix interaction in full $pf_{5/2}$ and $pf_{5/2}g_{9/2}$ model spaces, and the extended SU(3) model. Entries in parentheses show the result when only the normal spaces are used in the calculations.

$(J+2)^+ \rightarrow J^+$	$pf_{5/2}$	$pf_{5/2}g_{9/2}$	Ext. SU(3)	Exp [27]
$2^+_{g.s.} \rightarrow 0^+_{g.s.}$	257.22	253.91	292.80 (280.10)	410(60)
$4^+_{g.s.} \rightarrow 2^+_{g.s.}$	332.54	342.51	346.26 (334.10)	—
$6^+_{g.s.} \rightarrow 4^+_{g.s.}$	340.51	356.92	380.39 (370.56)	—
$8^+_{g.s.} \rightarrow 6^+_{g.s.}$	303.31	320.14	273.84 (268.08)	—
$4^+_\gamma \rightarrow 2^+_\gamma$	89.26	93.13	67.25 (65.73)	—
$6^+_\gamma \rightarrow 4^+_\gamma$	164.23	144.19	207.18 (204.78)	—
$8^+_\gamma \rightarrow 6^+_\gamma$	92.12	84.38	74.79 (79.39)	—
$(J+2)^+ \rightarrow J^+$	$pf_{5/2}$	$pf_{5/2}g_{9/2}$	Ext. SU(3)	Exp
$2^+_{g.s.} \rightarrow 0^+_{g.s.}$	322.71	314.66	354.17 (346.37)	—
$4^+_{g.s.} \rightarrow 2^+_{g.s.}$	448.07	440.68	486.65 (477.18)	—
$6^+_{g.s.} \rightarrow 4^+_{g.s.}$	441.58	435.77	473.89 (467.09)	—

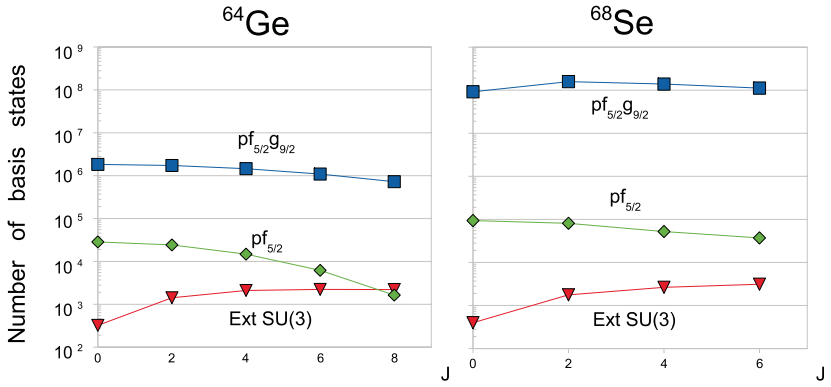

Figure 5. Model-space dimensions for calculations in the full $pf_{5/2}g_{9/2}$ space for ^{64}Ge and ^{68}Se as well as for the full $pf_{5/2}$ spaces and for the extended SU(3) shell model.

attributed to the fact that some of the states from this band (e.g. 4_2^+ and 6_2^+) are found to be highly mixed with $S = 1$ irreps and differ more significantly from the rest thus displaying a less regular structure pattern throughout the band, for example, to what has been observed in the same bands of some rare-earth nuclei. Results when only the normal-parity spaces are included in the calculation (shown in parentheses) reveal a contribution of the unique-parity sector of only up to 2-3%. An increase in this number is expected for higher-lying states or heavier nuclei where the dominant configurations are the ones with an occupied unique-parity space.

The content of the eigenstates from the g.s. ($K = 0^+$) band of ^{64}Ge shows dominance of the leading and most deformed SU(3) irrep $(8, 4)$ which gradually declines throughout the band from about 80% for $J = 0^+_{g.s.}$ to less than 40% for $J = 8^+_1$. Since the spin-orbit interaction is not as strong as in the case of the ds-shell nuclei, the mixing of irreps is smaller compared to the corresponding normal-SU(3) results for ^{24}Mg and ^{28}Si [7]. In the case of ^{68}Se, the leading irrep $(0, 12)$ contributes from 75 to 85% throughout the g.s. band.

Although the extended-SU(3) calculations are performed in a model space that involves the whole gds shell, the basis is still much smaller in size even compared with the one used for realistic calculations in the $pf_{5/2}g_{9/2}$ space. This drastic reduction translates into the use of only hundreds or at most a few thousand basis states (Figure 5). For example, the size of the basis used in the extended-SU(3) calculations for ^{64}Ge represents only between 0.02% to 0.3% of that for unrestricted calculations in the $pf_{5/2}g_{9/2}$ model space. This means that a space spanned by a set of extended-SU(3) basis states may be computationally manageable beyond the limit accessible for the modern full-space shell-model calculations as is the case for the combination of the upper-fp and the gds shells.

5 Conclusion

We extended the usual pseudo-SU(3) shell model for upper-fp shell nuclei in two ways: firstly by integrating the $g_{9/2}$ level into the dynamics; and secondly by including the entire gds-shell organized via its SU(3) structure, which we dubbed the extended SU(3) shell model. While this work only deals with the simplest case in which one configuration (the one with no particles in the unique-parity space) dominates all others, it is still possible to appreciate the strength of this new approach. Specifically, the model offers a richer model space compared to the previous SU(3) schemes by taking particles from the unique-parity space explicitly into account. As a result, the current approach presents an opportunity for a better description of the collectivity properties of the systems considered by reducing the effective charge needed in the description of their B(E2) transition strengths. These results will be even more pronounced for heavier systems where the intruder space is expected to have higher occupancy. This approach also offers an opportunity to explore the role of the intruder levels in the dynamics of the system as in the current study they are treated on the same footing as the normal-parity orbitals. It is important to underscore that these advantages are accomplished within a highly truncated and symmetry-adapted basis, which possibly allows one to reach into otherwise computationally challenging (if not inaccessible) domains.

The results for the nuclei ^{64}Ge and ^{68}Se demonstrate a close reproduction of various results obtained with a realistic interation. Specifically, many of the states in the energy spectra and the B(E2) transition strengths are nicely reproduced. While the results are satisfactory for the states from the g.s. bands, there still seem to be some need for a more precise description of the nuclear characteristics related to the properties of the eigenfunctions. These could be addressed in the future by including some corrections with the use of more elaborated interactions. Nevertheless, the results certainly suggest that the extended SU(3) model can be a valuable tool in studying properties of nuclei of special interest from this region, such as those lying close to the proton drip line or/and actively participating in the processes of nucleosynthesys. They also point to an excellent opportunity to reveal the role the intruder levels play in the dynamics of the system in an exciting and completely new way, namely, considering their connection to their like-parity partners within the framework of a severely-truncated symmetry-adapted model space.

Acknowledgements

This work is supported by the European Operational Program HRD through contract BGO051PO001/07/3.3-02/53 with the Bulgarian Ministry of Education and Science.

References

[1] J. Escher, J.P. Draayer, and A. Faessler, *Nucl. Phys.* **A586** (1995) 73.

[2] K.H. Bhatt, C.W. Nestor, Jr., and S. Raman, *Phys. Rev. C* **46** (1992) 164.

[3] K.H. Bhatt, S. Kahane, and S. Raman, *Phys. Rev. C* **61** (2000) 034317.

[4] S. Åberg, H. Flocard, and W. Nazarewicz, *Annu. Rev. Nucl. Part. Sci.* **40** (1990) 469.

[5] J.P. Elliott, *Proc. Roy. Soc. London, Ser. A* **245** (1958) 128; **A245** (1958) 562.

[6] R.D. Ratna Raju, J.P. Draayer, and K.T. Hecht, *Nucl. Phys.* **A202** (1973) 433.

[7] C. Vargas, J.G. Hirsch, and J.P. Draayer, *Nucl. Phys.* **A690** (2001) 409.

[8] C.E. Vargas, J.G. Hirsch, and J.P. Draayer, *Nucl. Phys.* **A697** (2002) 655.

[9] G. Popa, J.G. Hirsch, and J.P. Draayer, *Phys. Rev. C* **62** (2000) 064313; C. Vargas et al., *Phys. Rev. C* **61** (2000) 031301(R).

[10] H. Schatz et al., *Phys. Rep.* **294** (1998) 167; J.A. Clark et al., *Phys. Rev. C* **75** (2007) 032801(R).

[11] K. Kaneko, M. Hasegawa, and T. Mizusaki, *Phys. Rev. C* **C70** (2004) 051301(R).

[12] Y. Sun et al., *Nucl. Phys.* **A758** (2005) 765c.

[13] R.R. Whitehead et al., Adv. Nucl. Phys. 9 (1977) 123.

[14] E. Caurier et al., *Phys. Rev. Lett.* **77** (1996) 1954.

[15] A. Abzouzi, E. Caurier, and A.P. Zuker, *Phys. Rev. Lett.* **66** (1991) 1134; F. Nowacki, Ph. D. thesis, ULP Strasbourg, 1995 (unpublished).

[16] S.M. Vincent et al., *Phys. Lett.* **B437** (1998) 264.

[17] P. Van Isacker, O. Juillet, and F. Nowacki, *Phys. Rev. Lett.* **82** (1999) 2060.

[18] K.P. Drumev et al., to be submitted.

[19] R.R. Whitehead and A. Watt, *J. Phys. G* **4** (1978) 835; R.R. Whitehead et al., in *Theory and Application of moment methods in Many-Fermion systems*, edited by B. J. Dalton *et al.*., Plenum, New York (1980); E. Caurier, A. Poves, and A.P. Zuker, *Phys. Lett.* **B252** (1990) 13; *Phys. Rev. Lett.* **74** (1995) 1517.

[20] P. Ring and P. Schuck, *The Nuclear Many-Body Problem*, Springer, Berlin (1979).

[21] K. Kaneko, M. Hasegawa, and T. Mizusaki, *Phys. Rev. C* **66**, (2002) 051306(R).

[22] M. Dufour, A.P. Zuker, *Phys. Rev. C* **54** (1996) 1641.

[23] National Nuclear Data Center, http://www.nndc.bnl.gov.

[24] K.C. Tripathy and R. Sahu, *Int. Journ. Mod. Phys. E* **11** (2002) 531.

[25] S.M. Fischer et al., *Phys. Rev. Lett.* **84** (2000) 4064.

[26] J.P. Draayer and K.J. Weeks, *Ann. Phys. (N.Y.)* **156** (1984) 41; O. Castaños, J.P. Draayer, and Y. Leschber, *ibid.* **180** (1987) 290.

[27] K. Starosta et al., *Phys. Rev. Lett.* **99** (2007) 042503.